Palaeobiodiversity and Palaeoenvironments
https://doi.org/10.1007/s12549-021-00507-x

SENCKENBERG

ORIGINAL PAPER

Trepostome bryozoans buck the trend and ignore calcite-aragonite seas

Marcus M. Key Jr[1] · Patrick N. Wyse Jackson[2] · Catherine M. Reid[3]

Received: 28 April 2021 / Revised: 11 June 2021 / Accepted: 13 July 2021

Abstract

Trepostome bryozoan skeletalisation did not passively respond to changes in seawater chemistry associated with calcite-aragonite seas. According to Stanley and others, trepostome bryozoans were passive hypercalcifiers. However, if this was the case, we would expect their degree of calcitic colony calcification to have decreased across the Calcite I Sea to the Aragonite II Sea at its transition in the Middle Mississippian. Data from the type species of all 184 trepostome genera from the Early Ordovician to the Late Triassic were utilised to calculate the Bryozoan Skeletal Index (BSI) as a proxy for the degree of calcification. BSI values and genus-level diversity did not decrease across the transition from the Calcite I Sea to the Aragonite II Sea. Nor were there any changes in the number of genus originations and extinctions. This suggests that trepostome bryozoans were not passive hypercalcifiers but active biomineralisers that controlled the mineralogy and robustness of their skeletons regardless of changes in seawater chemistry.

Keywords Trepostomata · Bryozoa · Skeletalisation · Calcite-aragonite seas

Introduction

Stanley and Hardie (1998, 1999) synthesised a theory of temporal geochemical variation in the oceans through the Phanerozoic (last ~ 550 Myr), describing oscillations in the mineralogy of marine inorganic and biogenic carbonates, with intervals dominated by aragonite and/or high-Mg calcite (aragonite seas) and low-Mg calcite (calcite seas) (Sandberg 1975, 1983; Hardie 1996). They argued that temporal variation in the Mg/Ca ratio of seawater was driven by changes in plate tectonic spreading rates at mid-ocean ridges. Faster seafloor spreading lowers the Mg/Ca ratio in the oceans which favours biomineralisation of low-Mg calcite. The opposite creates aragonite conditions.

Their supporting data were derived from marine cements, ooids, evaporites, and tropical hypercalcifying organisms (e.g. calcareous green algae, sponges, and corals). This work has been subsequently supported by studies on coralline algae (Stanley et al. 2002), rugose corals (Webb and Sorauf 2002), crinoids (Dickson 2002, 2004), echinoids, crabs, shrimps, and serpulid worms (Ries 2004), as well as coccoliths (Stanley et al. 2005). This secular carbonate mineralogy model is also supported by oscillations in the composition of fluid inclusions in marine evaporites (Lowenstein et al. 2001), the Sr:Ca ratio of biogenic carbonate (Steuber and Veizer 2002), and bromine concentrations in halite (Siemann 2003). In contrast, others have argued that the secular pattern in carbonate mineralogy is controlled by oscillations in atmospheric pCO_2 (Mackenzie and Pigott 1981; Sandberg 1983; Wilkinson and Givens 1986; Burton and Walter 1991; Zhuravlev and Wood 2009). The debate over the driving mechanism continues (Montañez 2002; Schlager 2005; Ries 2010; van Dijk et al. 2016; Turchyn and DePaolo 2019).

Regardless of the causal process, if seawater chemistry changes are global in scope, then it might be expected that geochemical signals should be expressed beyond Stanley and Hardie's largely tropical examples and beyond these few

✉ Patrick N. Wyse Jackson
wysjcknp@tcd.ie

Marcus M. Key, Jr
key@dickinson.edu

[1] Department of Earth Sciences, Dickinson College, Carlisle, Pennsylvania 17013-2896, USA

[2] Patrick N. Wyse Jackson, Department of Geology, Trinity College, Dublin 2, Ireland

[3] Catherine M. Reid, School of Earth and Environment, University of Canterbury, Christchurch 8140, New Zealand

Published online: 09 October 2021

biogenic carbonate producers. If bryozoans are passive hypercalcifying animals, they could provide an independent test of these hypothesised temporal variations in seawater chemistry. Bryozoans are mineralogically variable (Smith et al. 1998). They have an excellent fossil record from the Ordovician to the present (Taylor 1993; Ernst 2020). They have adapted to a cool-water temperate to polar palaeolatitudinal distribution through the Phanerozoic (Taylor and Allison 1998). As colonial animals, they have at times been important hypercalcifying carbonate producers (Stanley and Hardie 1998, 1999; Stanley 2006).

Stanley and Hardie (1998, 1999), Stanley et al. (2002), and Montañez (2002) argue that seawater chemistry exerts a strong control on the biomineralogy of morphologically simple clades that have weak control over their calcification. In addition to algae, sponges, and corals, they explicitly mention bryozoans as an example. Stanley and Hardie (1998, 1999) and Stanley (2006) suggest the fossil abundance and degree of calcification of 'stony' stenolaemate bryozoans (i.e. trepostomes) were controlled by seawater chemistry because they were considered to be passive hypercalcifiers.

All trepostomes were calcitic (Taylor et al. 2010; Taylor 2020). While the detailed mineralogy of most trepostomes remains unknown, of those whose mineralogy has been determined, all were low-Mg calcite (LMC) with the exception of one, *Nicholsonella* from the Ordovician of North America, which was high-Mg calcite (Tavener-Smith and Williams 1972; Taylor and Wilson 1999; Smith et al. 2006). Assuming all trepostomes were LMC, we would predict their degree of calcification to be higher during the Calcite I Sea than the Aragonite II sea. If they are not significantly different, that suggests that bryozoans are able to actively biomineralise even in adverse conditions, thus are not passive as suggested by Stanley and others (Stanley and Hardie 1998, 1999; Stanley 2006). The fossil record of trepostomes overlaps with the Calcite I Sea-Aragonite II Sea transition which occurred in the Middle Mississippian of the Early Carboniferous. We will test the hypothesis that trepostomes were passive hypercalcifying animals by quantifying their degree of calcification across this transition.

Materials and methods

Trepostomes are an order of stenolaemate bryozoans which evolved in the early Ordovician and went extinct in the Late Triassic (Taylor 2020). Most abundant in the early Palaeozoic, they are informally known as 'stony bryozoans'. All species of trepostomes have long, tubular zooids. Although encrusting, massive, frondose, and bifoliate colonies occur, most are ramose with bifurcating cylindrical branches that form small bush-like colonies (Key et al. 2016). These branches have an inner thinner-walled endozone surrounded by a peripheral thicker-walled exozone (Fig. 1).

We used the Bryozoan Skeletal Index (BSI) developed by Wyse Jackson et al. (2020) as a proxy for the degree of calcification of the trepostomes. The BSI measures the relative proportion of skeletal carbonate to intrazoarial void space in stenolaemate bryozoan colonies. It is calculated from exozone width in longitudinal or transverse section (EW), zooecial wall thickness between adjacent autozooecial apertures in shallow

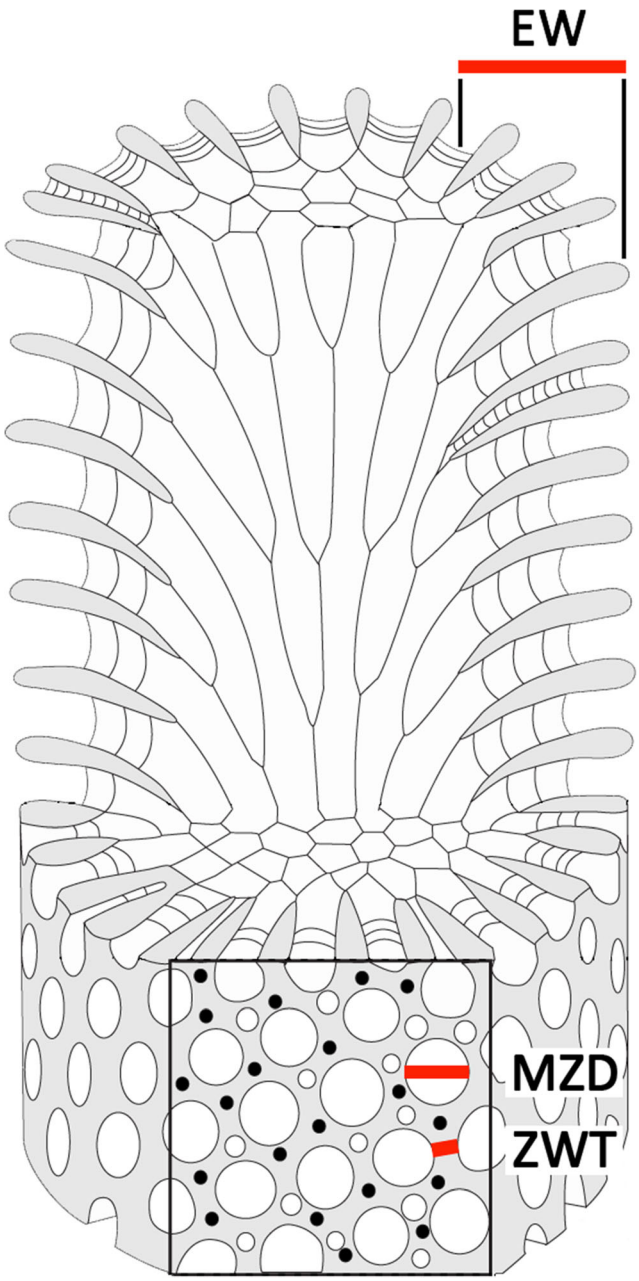

Fig. 1 Morphological characters used to compute the Bryozoan Skeletal Index (BSI). From Wyse Jackson et al. (2020, fig. 2). Abbreviations: EW, exozone width; MZD, autozooecial aperture diameter; ZWT, zooecial wall thickness

tangential section (ZWT), and autozooecial aperture diameter in shallow tangential section (MZD) using the following equation: BSI = ((EW × ZWT)/MZD) × 100 (Fig. 1). The multiplication factor of × 100 ensures that BSI is a whole number. Lower numbers represent lower levels of calcification and higher numbers the converse. For circular autozooecial apertures, the maximum MZD was measured. For oval-shaped apertures, both maximum and minimum MZD were determined and the average of the means of these used in the equation. For multilaminar encrusting species in which successive layers overgrow those immediately beneath, the thickness of the exozone in one lamina was measured.

We calculated BSI for the type species of each trepostome genus included in the forthcoming chapter on Order Trepostomata for the *Treatise on Invertebrate Paleontology*, Part G, Bryozoa, Revised, Volume 2 (Boardman and Buttler, forthcoming). We included all genera, regardless of their zoarial habit (Wyse Jackson et al. 2020, fig. 1). We determined the zoarial habit (i.e. ramose, encrusting, massive, foliose, bifoliate, or mixed) for each type species. When possible, we determined the zoarial habit from the type species' original publication and plates. For many species erected in the nineteenth century for which illustrations are either lacking or uninformative, we used the descriptions from the forthcoming *Treatise on Invertebrate Paleontology*'s trepostome volume (Boardman and Buttler, forthcoming). Our reliance on type specimens of type species of each genus assumes they are representative of the genus. They should be, as that is the fundamental purpose of type specimens and type species (ICZN 1999). But this approach requires the assumption that there is no significant intrageneric, intraspecific, or intracolony variation which is known to exist in bryozoans (Taylor 2020).

When possible, we acquired mean values for the three BSI morphometric parameters (EW, ZWT, MZD) from the type specimens of the type species of each genus. For more recently erected species, the morphometric data were extracted from published data tables. For older species descriptions lacking data tables, we used data from recent revisions of the taxa. Where means or ranges were not reported in the literature, replicate measurements for each parameter were taken directly from figured material accompanying the type descriptions or from the plates of Boardman and Buttler (forthcoming).

In some taxa, the dimensions of some parameters could not be determined from the type specimens of the type species. In these rare cases, it was measured from non-type material from the same species or from another species whose stratigraphic age and geographical location matched as closely as possible to those of the type species. This was mainly necessary for some taxa forming encrusting and massive zoaria in which the exozone width could not be accurately measured. In all such cases, the other parameter dimensions were compared with those of the type species to ensure that they were equivalent.

Type species ages were defined as the midpoint of the type locality stratigraphic age ranges from Shanan Peters' Macrostrat.org. Where type locality stratigraphic ages were not included in Macrostrat.org, we used updated stratigraphic concepts revised since the description of the species or local literature for some non-North American species. Genus stratigraphic ranges were based on the genus descriptions from Boardman and Buttler (forthcoming) and augmented with Phil Bock's Bryozoa.net. All numerical ages were based on the latest version of the ICS geologic time scale (Cohen et al. 2020).

We followed the methodology of Kiessling et al. (2008) and van Dijk et al. (2016) in using *t* tests to analyse for significant difference between the mean values before and after the Calcite I-Aragonite II transition. We used two approaches. The first examined BSI values across this transition using the midpoint of the age of the type species of each genus. The second used the stratigraphic range of each genus to look for a drop in the diversity of trepostomes across the transition.

Hardie (1996) put the Calcite I-Aragonite II transition date at 335 Ma based on the 1983 DNAG geologic time scale (Palmer 1983). Porter (2010, fig. 3), using a more recent geologic time scale (i.e. the 2008 ICS version whose Carboniferous boundary ages have not changed since then; Cohen et al. 2020), showed the transition date at 342 Ma. According to van Dijk et al. (2016), there is some disagreement about when the Calcite I-Aragonite II transition occurred. Depending on if one uses Stanley and Hardie's (1998, 1999) Mg/Ca model or Farkaš et al.'s (2007) Mg/Ca model, the estimated timing of transition ranges from 333 to 350 Ma (van Dijk et al. 2016, fig. 1). In contrast, Porter (2010, fig. 3) and Balthasar and Cusack (2015, fig. 2) suggest there is no period of uncertainty at this transition as opposed to the other transitions. Balthasar and Cusack (2015, fig. 2) and Quattrini et al. (2020, fig. 2) place it at 350 Ma. Therefore, we chose to test for changes to trepostome BSI across the transition at all three proposed ages of 333, 342, and 350 Ma.

Results

This study included all 184 trepostome genera (Table 1). They ranged from *Orbiramus* from the Tremadocian stage of the Early Ordovician of China to *Styloclema* from the Norian stage of the Late Triassic of New Zealand. That is an expanse of 265 Myr from 480 to 215 Ma (Fig. 2). The type species' BSI values ranged from 3 to 211 (mean: 44; standard deviation: 37) (Table 1). As determined by two sample *t* tests, there is no significant (i.e. $P > 0.05$) change in BSI values from before to after the 350 Ma mark, 342 Ma mark, or 333 Ma mark (Table 2). The mean BSI of all genera per 1 Myr bins across the ranges of all genera varied from 29 to 95 (mean: 53;

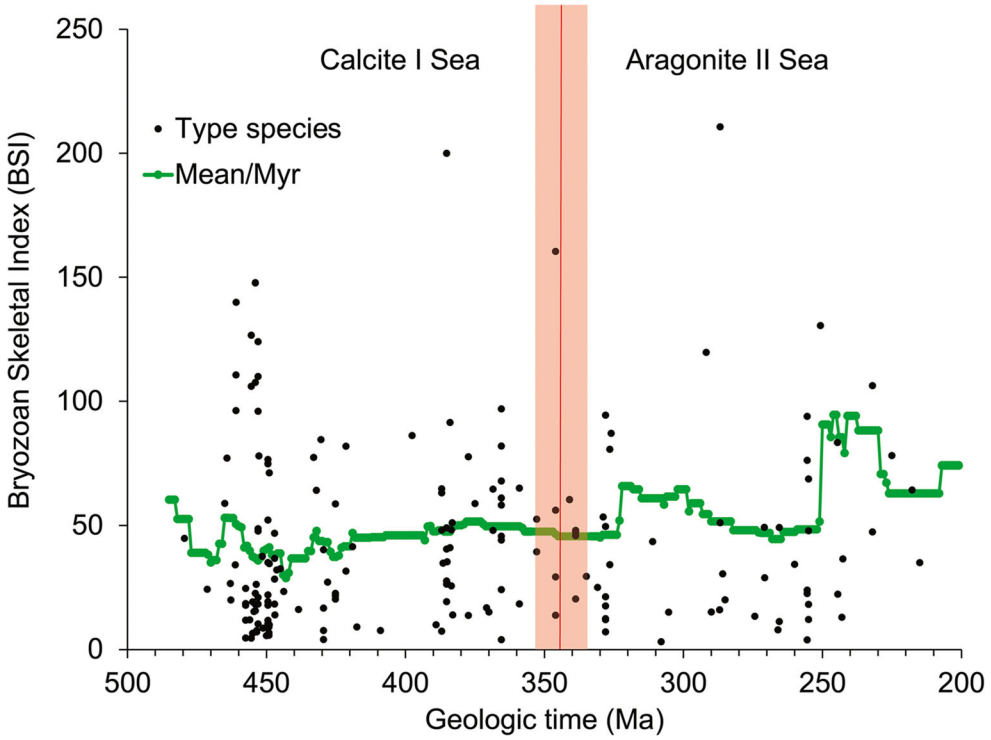

Fig. 2 Trepostome Bryozoan Skeletal Index (BSI) over geologic time based on each genus' type species mean age and the mean BSI per million years. Three different proposed ages for the transition from the Calcite I Sea to the Aragonite II Sea are shown by the shaded red box. Left edge of shaded box is 350 Ma, vertical line in centre is 342 Ma, and right edge of shaded box is 333 Ma

standard deviation: 14) (Fig. 2). There is essentially no change in mean BSI values at either the 350 Ma mark (47.5 before and after), 342 Ma mark (45.6 before and after), or 333 Ma (45.6 before and after).

Does the lack of change in BSI values hold up for individual zoarial types? There are not enough foliose and bifoliate trepostomes (n = 6), so they were excluded from this additional analysis. Genera whose type species are ramose or most commonly ramose (n = 125) showed no significant change in BSI across the Calcite I Sea/Aragonite II Sea transition, regardless of which of the three transition ages were chosen (two sample t-tests, $P > 0.05$, Table 2). Genera whose type species are encrusting or most commonly encrusting (n = 38) showed no significant change in BSI across the Calcite I Sea/Aragonite II Sea transition, regardless of which of the three transition ages were chosen (two sample *t* tests, $P > 0.05$, Table 2). Finally, genera whose type species are massive (n = 15) showed no significant change in BSI across the Calcite I Sea/Aragonite II Sea transition, regardless of which of the three transition ages were chosen (two sample *t* tests, $P > 0.05$, Table 2). Therefore, the pattern of lack of change in degree of calcification in response to changes in seawater chemistry is robust across each trepostome zoarial habit. Additionally, there is no change in genus-level trepostome diversity, originations, or extinctions across this transition (Fig. 3).

Discussion and conclusions

There was no significant decrease in BSI values as the calcitic trepostomes transitioned from the Calcite I Sea into the Aragonite II Sea (Table 2, Fig. 2). There was no change in diversity at either the 350 Ma mark (27 genera before and after), 342 Ma mark (26 genera before and after), or 333 Ma (26 genera before and after) (Fig. 3). In addition to the diversity graph being relatively flat during the transition, there was essentially no change in origination or extinction rate (Fig. 3). If trepostomes were responding to the changing ocean chemistry structurally, then one would expect new taxa to appear as trepostome systematics is based on skeletal structures. Trepostomes were structurally resilient to whatever was changing in seawater at the transition. If trepostomes were passive hypercalcifiers, then one would expect a drop in BSI values as the calcitic trepostomes transitioned from the Calcite I Sea into the Aragonite II Sea. If trepostomes were passive hypercalcifiers, then one could expect a macroevolutionary drop in diversity as the calcitic trepostomes transitioned from the Calcite I Sea into the Aragonite II Sea.

In contrast, two prominent diversity drops are visible in Fig. 3 and mark the mass extinctions defining the Ordovician-Silurian boundary (444 Ma; Sheehan 2001; Bond and Gasby 2020) and Permian-Triassic boundary (251

Table 1 Trepostome genera Bryozoan Skeletal Index (BSI) values, type species ages, and genera age ranges. Arranged by type species age.

Genus	Type species	Bryozoan Skeletal Index (BSI)	Type species age (Ma)	Lower range of genus (Ma)	Upper range of genus (Ma)
Styloclema	*morozovae*	35.0	215.0	227.0	208.5
Buria	*improvisa*	64.3	217.8	227.0	208.5
Metastenodiscus	*zealandicus*	78.1	225.0	227.0	201.3
Dyscritellopsis	*isoseptatus*	47.4	232.0	237.0	201.3
Zozariella	*stellata*	106.3	232.0	247.2	227.0
Phragmotrypa	*ordinata*	36.5	242.7	247.2	242.0
Reptonoditrypa	*cautica*	12.9	243.0	244.0	242.0
Tebitopora	*orientalis*	22.2	244.5	242.0	208.5
Vysokella	*acanthostylica*	83.4	244.6	247.2	242.0
Arcticopora	*christiei*	130.6	250.7	251.9	201.3
Iraidina	*damperovi*	47.9	255.0	259.1	251.9
Neoeridocampylus	*rarus*	68.8	255.0	259.1	251.9
Parastenodiscus	*nevolinae*	12.0	255.0	358.9	251.9
Ruzhencevia	*elegans*	18.1	255.0	273.0	251.9
Anisotrypella	*borealis*	76.2	255.5	259.1	251.9
Maychella	*tuberculata*	3.8	255.5	298.9	251.9
Permolioclema	*iraidae*	23.9	255.5	259.1	251.9
Permopora	*prima*	93.9	255.5	273.0	251.9
Ulrichotrypella	*kapitzae*	22.5	255.5	268.8	251.9
Araxopora	*spinigera var. araxensis*	34.3	260.0	298.9	251.9
Autospinifera	*rossae*	49.2	265.5	268.8	265.1
Stellahexaformis	*gersterensis*	11.2	265.5	273.0	251.9
Utgaardostylus	*stylata*	7.8	266.0	268.8	265.1
Neoeridotrypella	*pulchra*	28.9	270.8	290.1	251.9
Dyscritellina	*clivosa*	49.2	270.9	293.5	259.1
Crockfordia	*multinodata*	13.3	274.3	290.1	265.1
Toulapora	*svalbardensis*	20.0	285.0	293.5	283.5
Ulrichotrypa	*ramulosa*	30.4	285.9	298.9	251.9
Nansenopora	*peculiaris*	51.1	286.8	298.9	273.0
Stenodiscus	*moniliformis*	210.7	286.8	323.2	230.0
Paramaychellina	*spinosa*	16.0	287.0	298.9	251.9
Hinganella	*laeviuscula*	15.0	290.0	293.5	251.9
Stenopora	*tasmaniensis*	119.8	291.8	358.9	251.9
Crustoporella	*alekseevi*	14.9	305.4	307.0	303.7
Mishulgella	*stellata*	3.0	308.0	315.2	307.0
Rhombotrypella	*astragaloides*	43.5	311.1	323.2	251.9
Dunaevella	*shishovae*	87.1	326.0	330.9	319.0
Anisotrypa	*spinulosa*	80.6	326.5	427.4	323.2
Pseudobatostomella	*symmetrica*	34.1	326.5	419.2	201.3
Callocladia	*romingeri*	17.5	328.0	443.8	298.9
Coeloclemis	*tumida*	21.2	328.0	358.9	251.9
Dyscritella	*insigne*	94.4	328.0	419.2	201.3
Idioclema	*regularis*	49.6	328.0	358.9	323.2
Pycnopora	*frondosa*	7.0	328.0	358.9	323.2
Stenocladia	*robusta*	12.4	328.0	358.9	323.2
Stenoporella	*elegans*	11.9	328.0	330.9	323.2
Maychellina	*aliena*	53.4	328.9	358.9	251.9
Astralochoma	*helenae*	25.0	330.9	330.9	323.2
Nipponostenopora	*elegantula*	29.4	334.9	358.9	298.9
Hinaclema	*hinaensis*	45.9	338.8	358.9	283.5
Hunanopora	*lobatum*	48.0	338.8	358.9	323.2
Stenophragmidium	*sinensis*	20.3	338.8	346.7	330.9
Triznotrypa	*subtomiensis*	47.3	338.8	387.7	330.9
Leioclema	*concentrica*	60.4	341.0	485.4	201.3
Nikiforopora	*punctata*	60.5	341.0	358.9	298.9
Cyclopora	*fungia*	29.2	346.0	358.9	323.2
Proutella	*discoidea*	13.7	346.0	358.9	323.2
Tabulipora	*nalvkini*	56.2	346.0	419.0	251.9
Tabuliporella	*urii*	160.4	346.0	358.9	283.5
Raissiella	*bystrensis*	52.5	352.8	372.2	346.7
Volnovachia	*distincta*	39.4	352.8	358.9	323.2
Aisenvergia	*cylindrica*	65.1	359.0	358.9	346.7
Crustopora	*tuberculata*	18.3	359.0	407.6	323.2
Armillopora	*sinensis*	61.1	365.5	372.2	358.9

Table 1 (continued)

Genus	Type species	Bryozoan Skeletal Index (BSI)	Type species age (Ma)	Lower range of genus (Ma)	Upper range of genus (Ma)
Eodyscritella	*clathrata*	45.6	365.5	372.2	358.9
Fitzroyopora	*multiseptatum*	58.2	365.5	382.7	358.9
Granivallum	*shaodongensis*	68.0	365.5	382.7	358.9
Multiphragma	*hunanensis*	81.9	365.5	372.2	358.9
Polyspinopora	*granulosa*	96.9	365.5	372.2	358.9
Schulgina	*oscarensis*	44.1	365.5	382.7	358.9
Sinoatactotoechus	*fistulosum*	24.1	365.5	372.2	358.9
Triplopora	*nesterenkoae*	3.8	365.5	372.2	358.9
Hyalotoechus	*duncani*	48.0	368.5	379.0	358.0
Linotaxis	*magna*	64.7	368.5	379.0	358.0
Zefrehopora	*asynithis*	15.0	370.0	372.2	358.9
Percyopora	*tubulata*	16.7	370.8	382.7	358.9
Petalotrypa	*compressa*	58.9	375.0	393.3	382.7
Amplexoporella	*ornamentata*	77.6	377.4	382.7	372.2
Paralioclema	*ninae*	13.7	377.4	419.2	247.2
Atactotoechus	*typicus*	13.8	383.0	419.2	358.9
Kysylschinipora	*nekhoroschevi*	51.1	383.2	387.7	358.9
Dyoidophragma	*typicus*	25.6	383.5	393.3	358.9
Stereotoechus	*typicale*	48.2	383.5	391.0	379.0
Eostenopora	*picta*	91.4	384.0	388.0	379.0
Leptotrypella	*barrandi*	41.0	384.0	391.0	379.0
Eridocampylus	*ulrichi*	26.7	385.0	388.0	379.0
Microcampylus	*typicus*	35.3	385.0	388.0	379.0
Abakana	*macrospina*	49.0	385.2	387.7	382.7
Boardmanella	*richardi*	27.6	385.2	427.4	387.7
Diphragmoides	*paradoxus*	19.2	385.2	390.0	384.0
Eifelipora	*ramosa*	26.3	385.2	390.0	384.0
Minussina	*maculosa*	200.0	385.2	419.2	358.9
Neotrematopora	*typica*	40.4	385.2	427.4	330.0
Eridotrypella	*obliqua*	34.8	386.5	391.0	379.0
Loxophragma	*lechrium*	64.8	387.0	391.0	382.0
Polycylindricus	*amphelicta*	48.0	387.0	419.2	358.9
Pycnobasis	*asphinctus*	63.1	387.0	391.0	382.0
Trachytoechus	*typicus*	7.3	387.0	427.4	358.0
Multihemiphragma	*tenuis*	9.9	389.0	393.2	382.7
Mongoloclema	*ignotum*	86.2	397.6	407.6	387.7
Koneprusiella	*armata*	7.6	409.0	419.2	393.3
Badoglioporina	*parvulipora*	9.0	417.5	419.2	393.3
Diplostenopora	*siluriana*	41.4	419.0	422.0	413.0
Astroviella	*mukhovetskensis*	31.5	421.4	427.4	393.3
Astroviellina	*porosa*	81.9	421.4	423.0	419.2
Calamotrypa	*millichopensis*	20.2	425.2	427.4	423.0
Eridotrypellina	*insolens*	58.7	425.2	427.4	423.0
Hemieridotrypa	*tsherkesovae*	22.6	425.2	427.4	423.0
Pseudoleptotrypa	*podolica*	21.6	425.2	427.4	423.0
Hallopora	*elegantula*	27.1	428.0	458.4	393.3
Acanthotrypina	*spinosa*	3.9	429.5	433.4	427.4
Badogliopora	*ramulosum*	16.6	429.5	431.0	425.0
Leioclemina	*tuberculosa*	40.2	429.5	431.0	425.0
Trematopora	*spinulifera*	7.6	429.5	431.0	425.0
Diplotrypella	*densipora*	84.5	430.4	433.4	427.4
Asperopora	*aspera*	64.2	432.1	433.4	427.4
Idiotrypa	*parasitica*	77.3	433.0	431.0	425.0
Lioclemella	*ohioensis*	16.1	438.5	443.0	436.0
Canavaripora	*nitida*	23.4	443.8	457.0	434.0
Acanthotrypella	*variabile*	32.5	445.0	448.0	445.2
Jifarahpora	*lybiensis*	32.0	446.3	449.7	443.0
Rhombotrypa	*quadrata*	13.9	447.0	448.0	445.2
Anaphragma	*mirabile*	46.8	447.1	448.0	445.2
Calloporella	*harrisi*	28.3	447.1	448.0	445.2
Gortanipora	*crenulata*	18.3	447.1	456.0	445.2
Stigmatella	*bassleri*	36.7	447.1	451.0	445.2
Batostomella	*gracilis*	71.3	449.0	451.0	445.2
Leptotrypa	*ramosa*	9.9	449.0	458.4	443.8

Table 1 (continued)

Genus	Type species	Bryozoan Skeletal Index (BSI)	Type species age (Ma)	Lower range of genus (Ma)	Upper range of genus (Ma)
Parvohallopora	*minima*	34.5	449.0	453.0	445.2
Mesotrypa	*petechialis*	6.6	449.1	458.4	443.8
Peronopora	*decipiens*	9.0	449.1	457.0	442.0
Petigopora	*infida*	5.6	449.1	456.0	445.2
Amplexopora	*crassimuralis*	21.9	449.5	459.0	445.2
Bodywskites	*elegans*	10.4	449.5	461.2	449.2
Dekayia	*curvata*	19.2	449.5	457.0	445.2
Discotrypa	*mammulata*	11.7	449.5	451.0	447.0
Heterotrypa	*aspera*	76.5	449.5	459.0	445.2
Homotrypa	*septosa*	52.2	449.5	456.0	445.2
Monticulipora	*frondosa*	17.8	449.5	456.0	445.2
Ralfimartites	*fistulatus*	35.1	449.5	471.3	449.2
Tetratoechus	*lautus*	74.8	449.5	448.0	445.2
Lodenicella	*lamellata*	8.8	450.0	453.0	445.2
Bythopora	*dendrina*	5.5	450.1	470.0	443.8
Sonninopora	*tenuispinosa*	8.5	451.2	458.4	443.8
Polyteichus	*novaki*	37.5	451.5	453.0	448.0
Pedrogopora	*taylori*	77.9	452.7	458.4	449.3
Balticopora	*implicatum*	20.9	453.0	457.0	445.2
Balticoporella	*glabrum*	110.1	453.0	453.5	449.5
Batostoma	*mutabilis*	124.1	453.0	451.0	445.2
Cyphotrypa	*tenuimurale*	10.2	453.0	458.4	443.8
Eridotrypa	*typicalis*	47.7	453.0	456.0	430.0
Monotrypa	*acervulosa*	18.3	453.0	458.4	443.8
Newportopora	*undulata*	96.0	453.0	457.0	445.0
Nicholsonella	*ponderosa*	48.7	453.0	465.0	445.0
Dybowskites	*laxatus*	7.6	453.5	458.1	451.7
Nolvakites	*clavus*	7.0	453.5	454.0	453.0
Prasopora	*grayae*	26.2	453.7	458.4	443.8
Halloporina	*crenulata*	22.6	454.0	456.0	450.0
Hemiphragma	*instabilis*	147.8	454.0	465.0	445.2
Homotrypella	*aequalis*	107.7	454.0	457.0	445.2
Monotrypella	*irrasum*	18.1	454.0	457.0	450.0
Tarphophragma	*multitabulata*	15.6	454.0	465.0	445.0
Bimuropora	*dubia*	15.2	454.5	465.0	445.0
Atactopora	*typicalis*	19.2	455.0	458.4	443.8
Atactoporella	*hirsuta*	6.5	455.0	457.0	442.0
Diazipora	*monotrypoides*	4.5	455.5	467.3	452.0
Goldfussitrypa	*esthoniae*	106.1	455.5	458.4	449.0
Mesotrypina	*milleporacea*	126.7	455.5	457.0	454.0
Acantholaminatus	*typicus*	11.9	456.0	457.0	445.0
Aostipora	*sublamellosa*	24.5	457.5	470.0	445.2
Capillapora	*arcuata*	11.8	457.5	458.0	457.0
Orbignyella	*maculatum*	4.5	457.5	456.0	453.0
Phragmopora	*cystata*	18.5	457.5	470.0	443.8
Phragmoporella	*multiporarum*	17.8	457.5	463.0	456.0
Diplotrypa	*petropolitana*	140.0	460.9	467.3	443.8
Jordanopora	*heroensis*	110.7	461.0	465.0	456.0
Lamottopora	*duncanae*	96.2	461.0	465.0	456.0
Champlainopora	*chazyensis*	34.1	461.2	460.0	453.0
Rozhnovites	*limatus*	19.9	462.8	470.3	464.5
Kanoshopora	*droserae*	26.5	463.0	477.7	470.0
Trematoporina	*intercludens*	77.0	464.2	470.0	423.0
Eichwaldipora	*ovulum*	58.9	465.0	470.0	460.0
Dittopora	*claevaeformis*	24.2	471.3	477.7	433.4
Orbiramus	*normalis*	44.8	479.5	482.0	471.2

Ma; Erwin 2006; Li et al. 2021). Both had major impacts on bryozoan faunas globally (Taylor and Larwood 1988; Tuckey and Anstey 1992; Powers and Bottjer 2009; Taylor 2020).

Increased originations did lead to greater trepostome diversity and thus more scatter in BSI values (Fig. 2). This is best seen 460–455 Ma during the Great Ordovician Biodiversification

Table 2 Two sample *t* test statistics for trepostome Bryozoan Skeletal Index (BSI) values across the transition from the Calcite I Sea to the Aragonite II Sea by zoarial habit

	Age (Ma) of transition from Calcite I Sea to the Aragonite II Sea	350	342	333
All zoarial types	Calcite I Sea mean BSI	42.0	42.7	42.8
	Aragonite II Sea mean BSI	46.9	45.6	45.8
	Degrees of freedom	102	98	74
	t statistic	0.804	0.476	0.446
	P value	0.424	0.635	0.657
	Significant change from Calcite I Sea to the Aragonite II Sea based on $P < 0.05$?	No	No	No
Ramose zoaria	Calcite I Sea mean BSI	46.1	47.5	47.3
	Aragonite II Sea mean BSI	50.5	47.3	47.9
	Degrees of freedom	60	60	45
	t statistic	0.541	− 0.028	0.064
	P value	0.591	0.978	0.949
	Significant change from Calcite I Sea to the Aragonite II Sea based on $P < 0.05$?	No	No	No
Encrusting zoaria	Calcite I Sea mean BSI	22.9	22.8	23.7
	Aragonite II Sea mean BSI	35.8	37.9	37.2
	Degrees of freedom	26	20	17
	t statistic	1.509	1.650	1.400
	P value	0.143	0.114	0.180
	Significant change from Calcite I Sea to the Aragonite II Sea based on $P < 0.05$?	No	No	No
Massive zoaria	Calcite I Sea mean BSI	49.3	49.3	49.3
	Aragonite II Sea mean BSI	56.9	56.9	56.9
	Degrees of freedom	5	5	5
	t statistic	0.285	0.285	0.285
	P value	0.787	0.787	0.787
	Significant change from Calcite I Sea to the Aragonite II Sea based on $P < 0.05$?	No	No	No

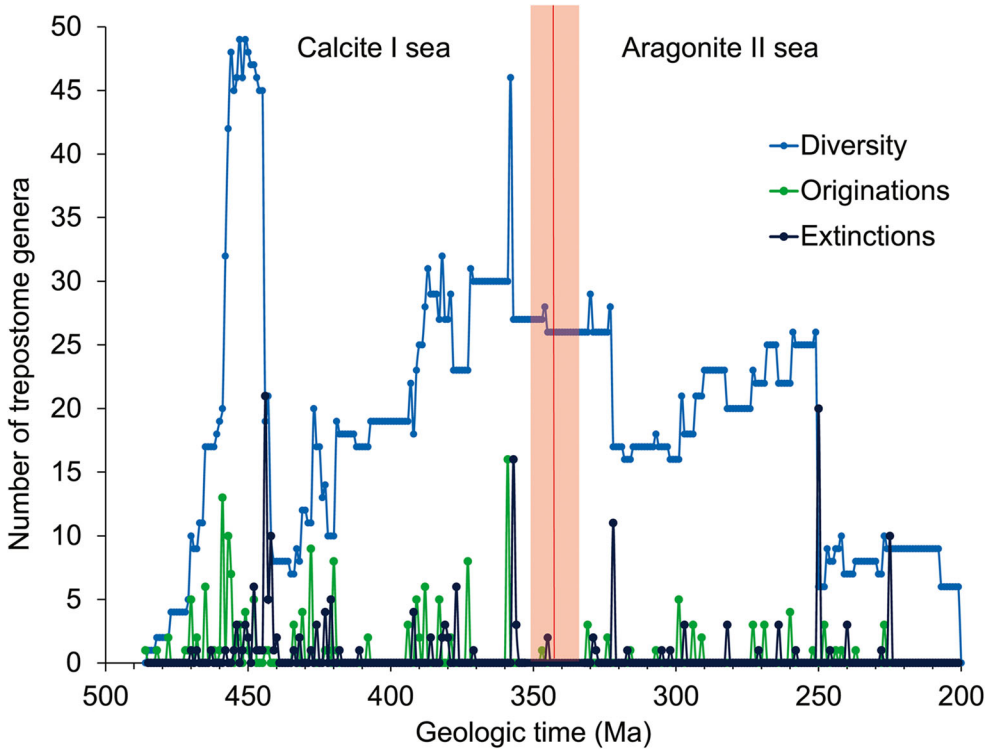

Fig. 3 Trepostome genus diversity and number of originations and extinctions over geologic time based on the stratigraphic range of each genus. Three different proposed ages for the transition from the Calcite I Sea to the Aragonite II Sea are shown by the shaded red box. Left edge of red box is 350 Ma, vertical red line in centre is 342 Ma, and right edge of shaded box is 333 Ma

Event (GOBE) (Webby et al. 2004). The combination of increased diversity and BSI values may have contributed to bryozoans being the most diverse group of reef-building organisms during the GOBE (Ernst 2018; Servais and Harper 2018). The Ordovician diversification of trepostomes was a component of the GOBE (Taylor and Larwood 1990; Taylor and Ernst 2004), including as a substrate for the Ordovician Bioerosion Revolution (Mángano et al. 2016).

The lack of change from the Calcite I Sea into the Aragonite II Sea suggests that the trepostomes were accommodating the change in seawater chemistry in some other way. Laboratory experiments on extant passive aragonite and calcite biomineralisers grown in the different seawater Mg/Ca ratios (Ries 2005; Stanley et al. 2010; Mewes et al. 2014) suggest that passive biomineralisers respond to unfavourable seawater conditions by changing skeletal composition. Thus, the calcitic trepostomes would have been using more energy to precipitate their skeletons in the less favourable seawater chemistry in the Aragonite II Sea, so they may have actively channelled more resources to calcification. Alternatively, they may have been dealing with the changing ocean chemistry metabolically or reproductively, not structurally as evidenced in the BSI. The fact that there was no change in BSI values, diversity, originations, or extinctions at the Calcite I Sea transition into the Aragonite II Sea provides strong evidence that trepostomes were not passive hyper-calcifiers but actively managed their calcification.

From a mineralogy perspective, modern bryozoans are not passive biomineralisers. They can precipitate a mix of LMC, HMC, and aragonite where needed in their skeletons tailored to the functional needs of the colonies (Smith et al. 2006; Taylor et al. 2009). Thus, they are best described as active biomineralisers. This has been previously argued for the post-Palaeozoic cheilostomes (Smith et al. 2006; Taylor et al. 2009) and the Palaeozoic trepostomes (Taylor and Kuklinski 2011).

In Taylor and Kuklinski's (2011) study, they used two independent proxies (i.e. branch diameter and ZWT) for degree of calcification in trepostomes. We used BSI which incorporates three parameters including exozone width instead of branch diameter which is composed of the highly calcified exozone and the minimally calcified endozone. They looked only at dendroid (i.e. ramose) forms, whereas we included all zoarial habits. They compiled their data from the literature for 188 species in 44 genera from the Ordovician (calcite sea), Devonian (calcite sea), and Permian (aragonite sea), whereas we included all genera and the entire trepostome stratigraphic range from the Ordovician to the Triassic and all periods in between. Despite these differences in sample size and range, our results were similar. Trepostome calcification did not alter in response to changes in the Mg/Ca ratio of seawater. Factors other than ocean chemistry control their calcification. Trepostomes, and likely all bryozoans, are active biomineralisers, not passive hypercalcifiers.

Acknowledgements Robert S. Nelson, III, collected some of this data as part of his senior thesis at Dickinson College. Caroline Buttler provided access to the genus descriptions and plates for the forthcoming Trepostome volume of the Treatise. This manuscript was greatly improved by the thoughtful reviews of Andrej Ernst and Abigail Smith.

Funding Open Access funding provided by the IReL Consortium.

Declarations

Conflict of interest The authors declare that they have no conflict of interest.

References

Balthasar, U., & Cusack, M. (2015). Aragonite-calcite seas–Quantifying the gray area. *Geology, 43*, 99–102. https://doi.org/10.1130/G36293.1.

Bond, D. P. G., & Gasby, S. E. (2020). Late Ordovician mass extinction caused by volcanism, warming, and anoxia, not cooling and glaciation. *Geology, 48*, 777–781. https://doi.org/10.1130/G47377.1.

Burton, E. A., & Walter, L. M. (1991). The effects of PCO_2 and temperature on magnesium incorporation in calcite in seawater and $MgCl_2$-$CaCl_2$ solutions. *Geochimica et Cosmochimica Acta, 55*, 777–785. https://doi.org/10.1016/0016-7037(91)90341-2.

Cohen, K. M., Harper, D. A. T., Gibbard, P. L., & Fan, J.-X. (2020). *The ICS international chronostratigraphic chart* (version 2020/03). International Commission on Stratigraphy. Retrieved February 14 2021 from https://stratigraphy.org/ICSchart/ChronostratChart2020-03.pdf

Dickson, J. A. D. (2002). Fossil echinoderms as monitor of the Mg/Ca ratio of Phanerozoic oceans. *Science, 298*, 1222–1224. https://doi.org/10.1306/112203740355.

Dickson, J. A. D. (2004). Echinoderm skeletal preservation: Calcite-aragonite seas and the Mg/Ca ratio of Phanerozoic oceans. *Journal of Sedimentary Research, 74*, 355–365. https://doi.org/10.1306/112203740355.

Dijk, I. van, de Nooijer, L. J., Hart, M. B., & Reichart, G.-J. (2016). The long-term impact of magnesium in seawater on foraminiferal mineralogy: Mechanism and consequences. *Global Biogeochemical Cycles, 30*, 438–446. https://doi.org/10.1002/2015GB005241.

Ernst, A. (2018). Diversity dynamics of Ordovician bryozoa. *Lethaia, 51*, 198–206. https://doi.org/10.1111/let.12235.

Ernst, A. (2020). 2. Fossil record and evolution of Bryozoa. In T. Schwaha (Ed.), *Phylum Bryozoa* (pp. 11–55). De Gruyter. https://doi.org/10.1515/9783110586312-002.

Erwin, D. H. (2006). *Extinction: How life on earth nearly ended 250 million years ago*. Princeton University Press ISBN 0-691-00524-9.

Farkaš, J., Böhm, F., Wallmann, K., Blenkinsop, J., Eisenhauer, A., van Geldern, R., Munnecke, A., Voigt, S., & Veizer, J. (2007). Calcium isotope record of Phanerozoic oceans: Implications for chemical evolution of seawater and its causative mechanisms. *Geochimica et Cosmochimica Acta, 71*, 5117–5134. https://doi.org/10.1016/j.gca.2007.09.004.

Hardie, L. A. (1996). Secular variation in seawater chemistry: An explanation for the coupled secular variation in the mineralogies of marine limestones and potash evaporites over the past 600 m.y. *Geology, 24*, 279–283. https://doi.org/10.1130/0091-7613(1996)024<0279:SVISCA>2.3.CO;2.

ICZN. (1999). *International code of zoological nomenclature*. International Commission on Zoological Nomenclature ISBN 0-85301-006-4.

Key Jr., M. M., Wyse Jackson, P. N., & Felton, S. H. (2016). Intracolony variation in colony morphology in reassembled fossil ramose stenolaemate bryozoans from the Upper Ordovician (Katian) of the Cincinnati Arch region, USA. *Journal of Paleontology, 90*, 400–412. https://doi.org/10.1017/jpa.2016.66.

Kiessling, W., Aberhan, M., & Villier, L. (2008). Phanerozoic trends in skeletal mineralogy driven by mass extinctions. *Nature Geoscience, 1*, 527–530. https://doi.org/10.1038/ngeo251.

Li, M., Grasby, S. E., Wang, S.-J., Zhang, X., Wasylenki, L. E., Xu, Y., Sun, M., Beauchamp, B., Hu, D., & Shen, Y. (2021). Nickel isotopes link Siberian traps aerosol particles to the end-Permian mass extinction. *Nature Communications, 12*, 2024. https://doi.org/10.1038/s41467-021-22066-7.

Lowenstein, T. K., Timofeeff, M. N., Brennan, S. T., Hardie, L. A., & Demicco, R. V. (2001). Oscillations in Phanerozoic seawater chemistry: Evidence from fluid inclusions. *Science, 294*, 1086–1088. https://doi.org/10.1126/science.1064280.

Mackenzie, F. T., & Pigott, J. D. (1981). Tectonic controls of Phanerozoic sedimentary rock cycling. *Journal of the Geological Society, 138*, 183–196. https://doi.org/10.1144/gsjgs.138.2.0183.

Mángano, M. G., Buatois, L. A., Wilson, M., & Droser, M. (2016). The great Ordovician biodiversification event. In M. G. Mángano & L. A. Buatoi (Eds.), *The trace-fossil record of major evolutionary events* (pp. 127–156). Springer, Topics in Geobiology 39. https://doi.org/10.1007/978-94-017-9600-2_4.

Mewes, A., Langer, G., Jan de Nooijer, L., Bijma, J., & Reichart, G.-J. (2014). Effect of different seawater Mg^{2+} concentrations on calcification in two benthic foraminifers. *Marine Micropaleontology, 113*, 56–64. https://doi.org/10.1016/j.marmicro.2014.09.003.

Montañez, I. P. (2002). Biological skeletal carbonate records changes in major-ion chemistry of paleo-oceans. *Proceedings of the National Academy of Sciences, 99*, 15,852–15,854. https://doi.org/10.1073/pnas.262659599.

Palmer, A. R. (1983). The decade of North American geology 1983 geologic time scale. *Geology, 11*, 503–504. https://doi.org/10.1130/0091-7613(1983)11<503:TDONAG>2.0.CO;2.

Porter, S. M. (2010). Calcite and aragonite seas and the *de novo* acquisition of carbonate skeletons. *Geobiology, 8*, 256–277. https://doi.org/10.1111/j.1472-4669.2010.00246.x.

Powers, C. M., & Bottjer, D. J. (2009). Behavior of lophophorates during the end-Permian mass extinction and recovery. *Journal of Asian Earth Sciences, 36*, 413–419. https://doi.org/10.1016/j.jseaes.2008.05.002.

Quattrini, A. M., Rodríguez, E., Faircloth, B. C., Cowman, P. F., Brugler, M. R., Farfan, G. A., Hellberg, M. E., Kitahara, M. V., Morrison, C. L., Paz-García, D. A., Reimer, J. D., & McFadden, C. S. (2020). Palaeoclimate ocean conditions shaped the evolution of corals and their skeletons through deep time. *Nature Ecology & Evolution, 4*, 1531–1538. https://doi.org/10.1038/s41559-020-01291-1.

Ries, J. B. (2004). Effect of ambient Mg/Ca ratio on Mg fractionation in calcareous marine invertebrates: A record of the oceanic Mg/Ca ratio over the Phanerozoic. *Geology, 32*, 981–984. https://doi.org/10.1130/G20851.1.

Ries, J. B. (2005). Aragonite production in calcite seas: Effect of seawater Mg/Ca ratio on calcification and growth of the calcareous alga *Penicillus capitatus*. *Paleobiology, 31*, 445–458. https://doi.org/10.1666/0094-8373(2005)031[0445:APICSE]2.0.CO;2.

Ries, J. B. (2010). Review: Geological and experimental evidence for secular variation in seawater Mg/Ca (calcite-aragonite seas) and its effects on marine biological calcification. *Biogeosciences, 7*, 2795–2849. https://doi.org/10.5194/bg-7-2795-2010.

Sandberg, P. A. (1975). New interpretations of Great Salt Lake ooids and of ancient nonskeletal carbonate mineralogy. *Sedimentology, 22*, 497–537. https://doi.org/10.1111/j.1365-3091.1975.tb00244.x.

Sandberg, P. A. (1983). An oscillating trend in Phanerozoic non-skeletal carbonate mineralogy. *Nature, 305*, 19–22. https://doi.org/10.1038/305019a0.

Schlager, W. (2005). Secular oscillations in the stratigraphic record - an acute debate. *Facies, 51*, 13–17. https://doi.org/10.1007/s10347-005-0066-5.

Servais, T., & Harper, D. A. T. (2018). The great Ordovician biodiversification event (GOBE): Definition, concept and duration. *Lethaia, 51*, 151–164. https://doi.org/10.1111/let.12259.

Sheehan, P. M. (2001). The Late Ordovician mass extinction. *Annual Review of Earth and Planetary Sciences, 29*, 331–364. https://doi.org/10.1146/annurev.earth.29.1.331.

Siemann, M. G. (2003). Extensive and rapid changes in seawater chemistry during the Phanerozoic: Evidence from Br contents in basal halite. *Terra Nova, 15*, 243–248. https://doi.org/10.1046/j.1365-3121.2003.00490.x.

Smith, A. M., Nelson, C. S., & Spencer, H. G. (1998). Skeletal carbonate mineralogy of New Zealand bryozoans. *Marine Geology, 151*, 27–46. https://doi.org/10.1016/S0025-3227(98)00055-3.

Smith, A. M., Key Jr., M. M., & Gordon, D. P. (2006). Skeletal mineralogy of bryozoans: Taxonomic and temporal patterns. *Earth Science Reviews, 78*, 287–306. https://doi.org/10.1016/j.earscirev.2006.06.001.

Stanley, S. M. (2006). Influence of seawater chemistry on biomineralization throughout Phanerozoic time: Paleontological and experimental evidence. *Palaeogeography, Palaeoclimatology, Palaeoecology, 232*, 214–236. https://doi.org/10.1016/j.palaeo.2005.12.010.

Stanley, S. M., & Hardie, L. A. (1998). Secular oscillations in the carbonate mineralogy of reef-building and sediment-producing organisms driven by tectonically forced shifts in seawater chemistry. *Palaeogeography, Palaeoclimatology, Palaeoecology, 144*, 3–19. https://doi.org/10.1016/S0031-0182(98)00109-6.

Stanley, S. M., & Hardie, L. A. (1999). Hypercalcification: Paleontology links plate tectonics and geochemistry to sedimentology. *GSA Today, 9*, 1–7.

Stanley, S. M., Ries, J. B., & Hardie, L. A. (2002). Low-magnesium calcite produced by coralline algae in seawater of Late Cretaceous composition. *Proceedings of the National Academy of Sciences, 99*, 15323–15326. https://doi.org/10.1073/pnas.232569499.

Stanley, S. M., Ries, J. B., & Hardie, L. A. (2005). Seawater chemistry, coccolithophore population growth, and the origin of Cretaceous chalk. *Geology, 33*, 593–596. https://doi.org/10.1130/G21405.1.

Stanley, S. M., Ries, J. B., & Hardie, L. A. (2010). Increased production of calcite and slower growth for the major sediment-producing alga *Halimeda* as the Mg/Ca ratio of seawater is lowered to a "calcite sea" level. *Journal of Sedimentary Research, 80*, 6–16. https://doi.org/10.2110/jsr.2010.011.

Steuber, T., & Veizer, J. (2002). Phanerozoic record of plate tectonic control of seawater chemistry and carbonate sedimentation. *Geology, 30*, 1123–1126. https://doi.org/10.1130/0091-7613(2002)030<1123:PROPTC>2.0.CO;2.

Tavener-Smith, R., & Williams, A. (1972). The secretion and structure of the skeleton of living and fossil Bryozoa. *Philosophical Transactions of the Royal Society of London, B, Biological Sciences, 264*, 97–159. https://doi.org/10.1098/rstb.1972.0010.

Taylor PD (1993) Bryozoa. In. M. J. Benton (Ed.), *The fossil record 2* (pp. 465–489). Chapman and Hall.

Taylor, P. D. (2020). *Bryozoan paleobiology*. Wiley Blackwell.

Taylor, P. D., & Allison, P. A. (1998). Bryozoan carbonates through time and space. *Geology, 26*, 459–462. https://doi.org/10.1130/0091-7613(1998)026<0459:BCTTAS>2.3.CO;2.

Taylor, P. D., & Ernst, A. (2004). Bryozoan diversification during the Ordovician. In B. D. Webby, M. L. Droser, & F. Paris (Eds.), The Great Ordovician Biodiversification Event (pp. 147–156). Columbia University Press.

Taylor, P. D., & Kuklinski, P. (2011). Seawater chemistry and biomineralization: Did trepostome bryozoans become hypercalcified in the 'calcite sea' of the Ordovician? *Palaeobiodiversity and Palaeoenvironments, 91*(3), 185–195. https://doi.org/10.1007/s12549-011-0054-4.

Taylor, P. D., & Larwood, G. P. (1988). Mass extinctions and the pattern of bryozoan evolution. In G. P. Larwood (Ed.), *Extinction and Survival in the Fossil Record (pp. 99–119)*. Systematics Association.

Taylor, P. D., & Larwood, G. P. (1990). Major evolutionary radiations in the Bryozoa. In P. D. Taylor & G. P. Larwood (Eds.), *Major Evolutionary Radiations (pp. 209–233)*. Systematics Association.

Taylor, P. D., & Wilson, M. A. (1999). *Dianulites* Eichwald, 1829: An unusual Ordovician bryozoan with a high-magnesium calcite skeleton. *Journal of Paleontology, 73*, 38–48. https://doi.org/10.1017/S0022336000027529.

Taylor, P. D., James, N. P., Bone, Y., Kuklinski, P., & Kyser, T. K. (2009). Evolving mineralogy of cheilostome bryozoans. *Palaios, 24*, 440–452. https://doi.org/10.2110/palo.2008.p08-124r.

Taylor, P. D., Vinn, O., & Wilson, M. A. (2010). Evolution of biomineralization in lophophorates. *Special Papers in Palaeontology, 84*, 317–333. https://doi.org/10.1111/j.1475-4983.2010.00985.x.

Tuckey, M. E., & Anstey, R. L. (1992). Late Ordovician extinctions of bryozoans. *Lethaia, 25*, 111–117. https://doi.org/10.1111/j.1502-3931.1992.tb01795.x.

Turchyn, A. V., & DePaolo, D. J. (2019). Seawater chemistry through Phanerozoic time. *Annual Review of Earth and Planetary Sciences, 47*, 197–224. https://doi.org/10.1146/annurev-earth-082517-010305.

Webb, G. E., & Sorauf, J. E. (2002). Zigzag microstructure in rugose corals: A possible indicator of relative seawater Mg/Ca ratios. *Geology, 30*, 415–418. https://doi.org/10.1130/0091-7613(2002)030<0415:ZMIRCA>2.0.CO;2.

Webby, B. D., Droser, M. L., Paris, F., & Percival, I. G. (2004). The great Ordovician biodiversification event. Columbia University Press.

Wilkinson, B. H., & Givens, K. R. (1986). Secular variation in abiotic marine carbonates: Constraints on Phanerozoic atmospheric carbon dioxide contents and oceanic Mg/Ca ratios. *Journal of Geology, 94*, 321–333. https://doi.org/10.1086/629032.

Wyse Jackson, P. N., Key Jr., M. M., & Reid, C. M. (2020). Bryozoan skeletal index (BSI): A measure of the degree of calcification in stenolaemate bryozoans. In P. N. Wyse Jackson & K. Zagorsek (Eds.), *Bryozoan Studies 2019* (pp. 193–206). Czech Geological Survey.

Zhuravlev, A. Y., & Wood, R. A. (2009). Controls on carbonate skeletal mineralogy: Global CO_2 evolution and mass extinctions. *Geology, 37*, 1123–1126. https://doi.org/10.1130/G30204A.1.